Effects of Vegetation Fraction Variation on Regional Climate Simulation over Eastern China

Yan Yan, Jianping Tang

School of Atmospheric Science

Nanjing University, Nanjing, China

ICRC-CORDEX 2019 16th Oct Beijing

Session B1: Atmosphere-land

Outline

- Background & History
- Vegetation Effects over China
- Conclusions

Outline

- Background & History
- Vegetation Effects over China
- Conclusions

Notaro et al., 2006

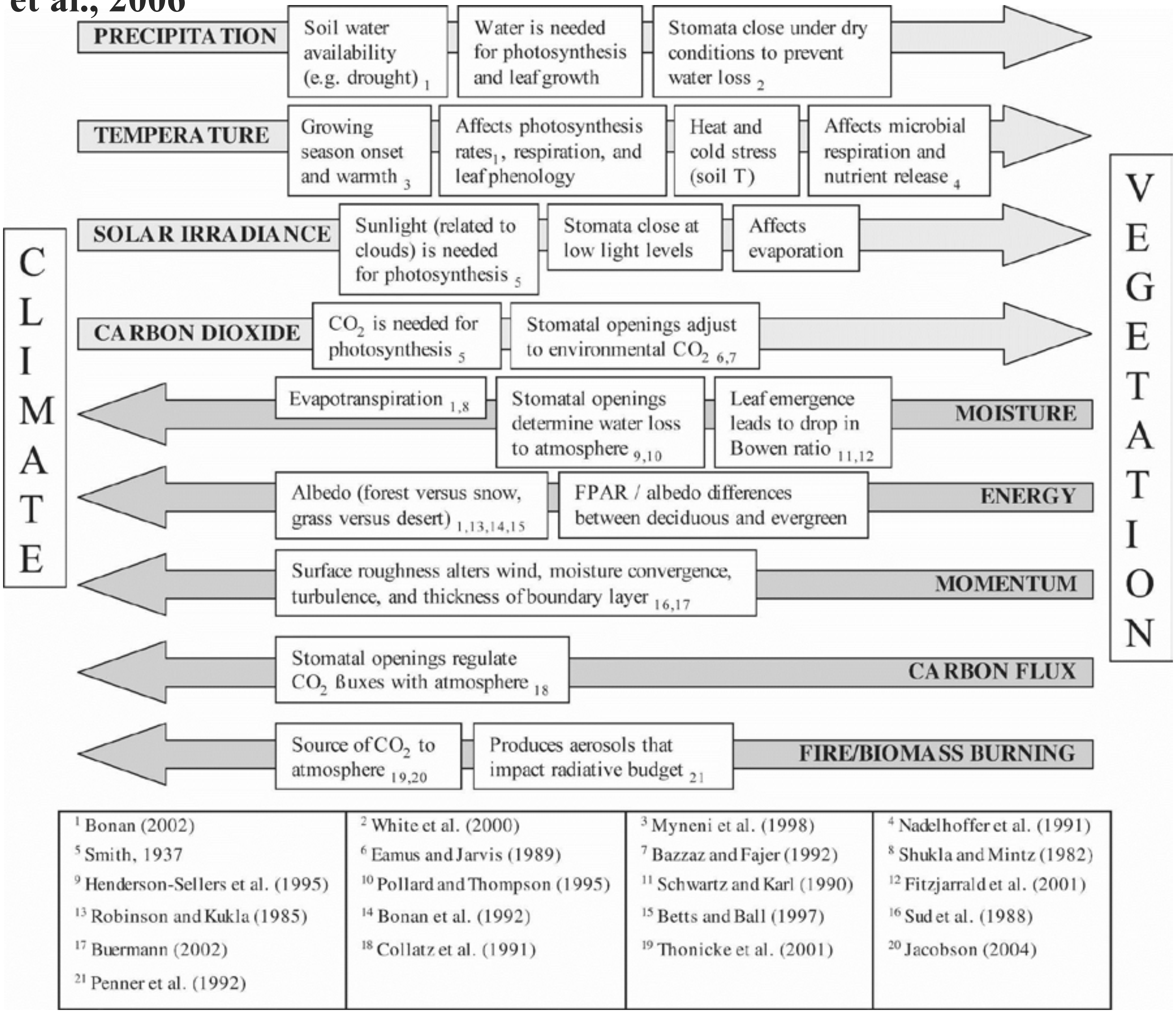

Forzieri et al., 2017

The remotely sensed dynamics in leaf area index (LAI) shows the interplay between LAI and surface biophysics is amplified up to 5 times under extreme warm-dry and cold-wet years.

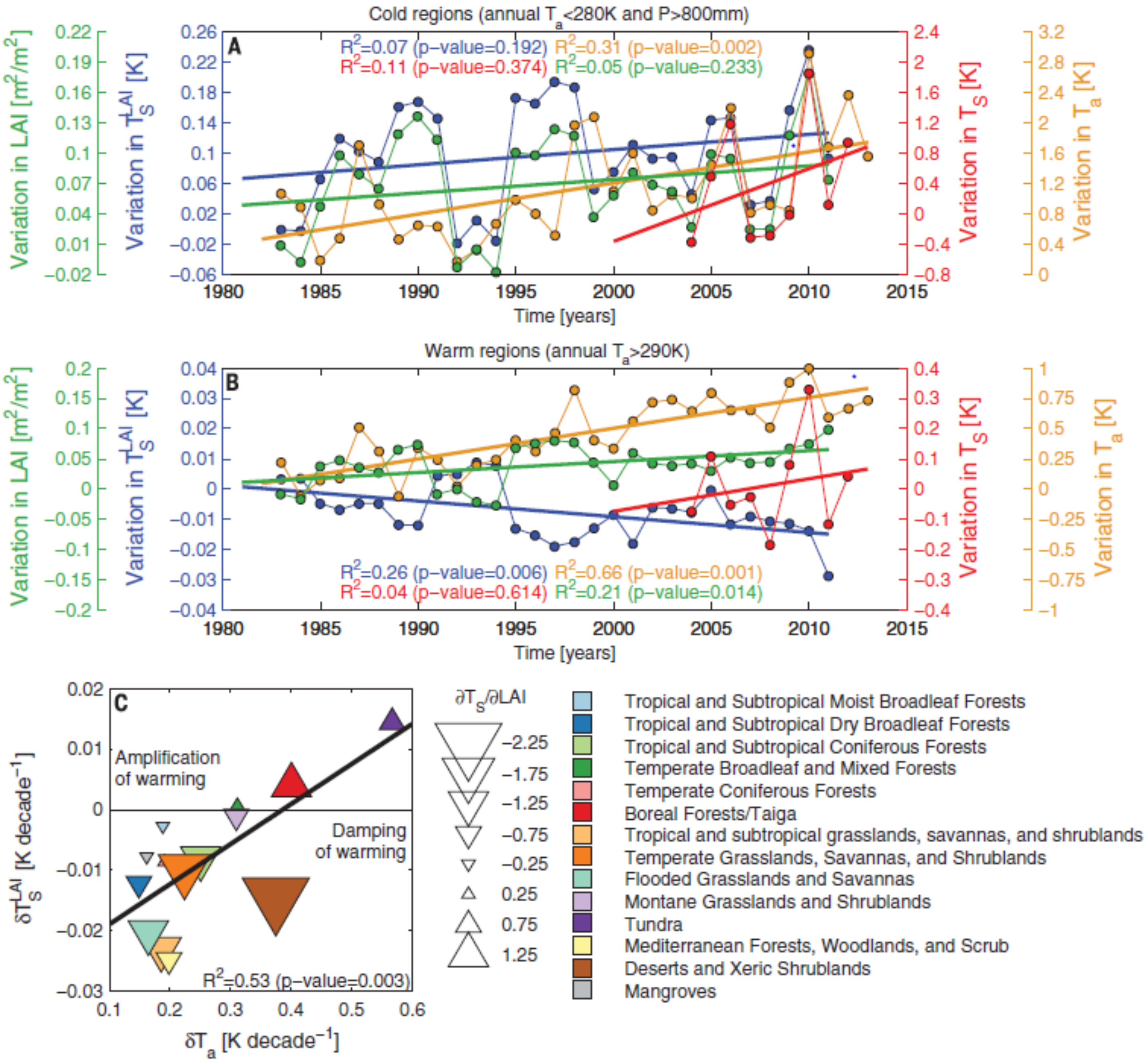

Fig. 4. Biophysical effects of the global greening on recent temperature trends. (**A**) Variation in LAI, LAI-related surface temperature (T_S^{LAI}), overall land surface temperature (T_S), and air temperature (T_a) expressed with respect to the first observational year (1982) and spatially aggregated over cold-wet regions (annual $T_a < 280$ K and $P > 800$ mm). Regression lines are overlaid for each variable, and corresponding coefficients of determination are reported in the label (supplementary text S7, materials and methods). (**B**) As (A), but for warm regions (annual $T_a > 290$ K). (**C**) Relations between the long-term trend in air temperature (δT_a, on the x axis) and the LAI-related trend in surface temperature (δT_S^{LAI}, on the y axis) spatially aggregated for different biomes. Upward- and downward-pointing triangles indicate positive and negative sensitivity of T_S to LAI ($\frac{\partial T_S}{\partial LAI}$), respectively. The size of the triangle refers to absolute value of sensitivity. Spatial domains of biomes are shown in fig. S6.

Notaro et al., 2017

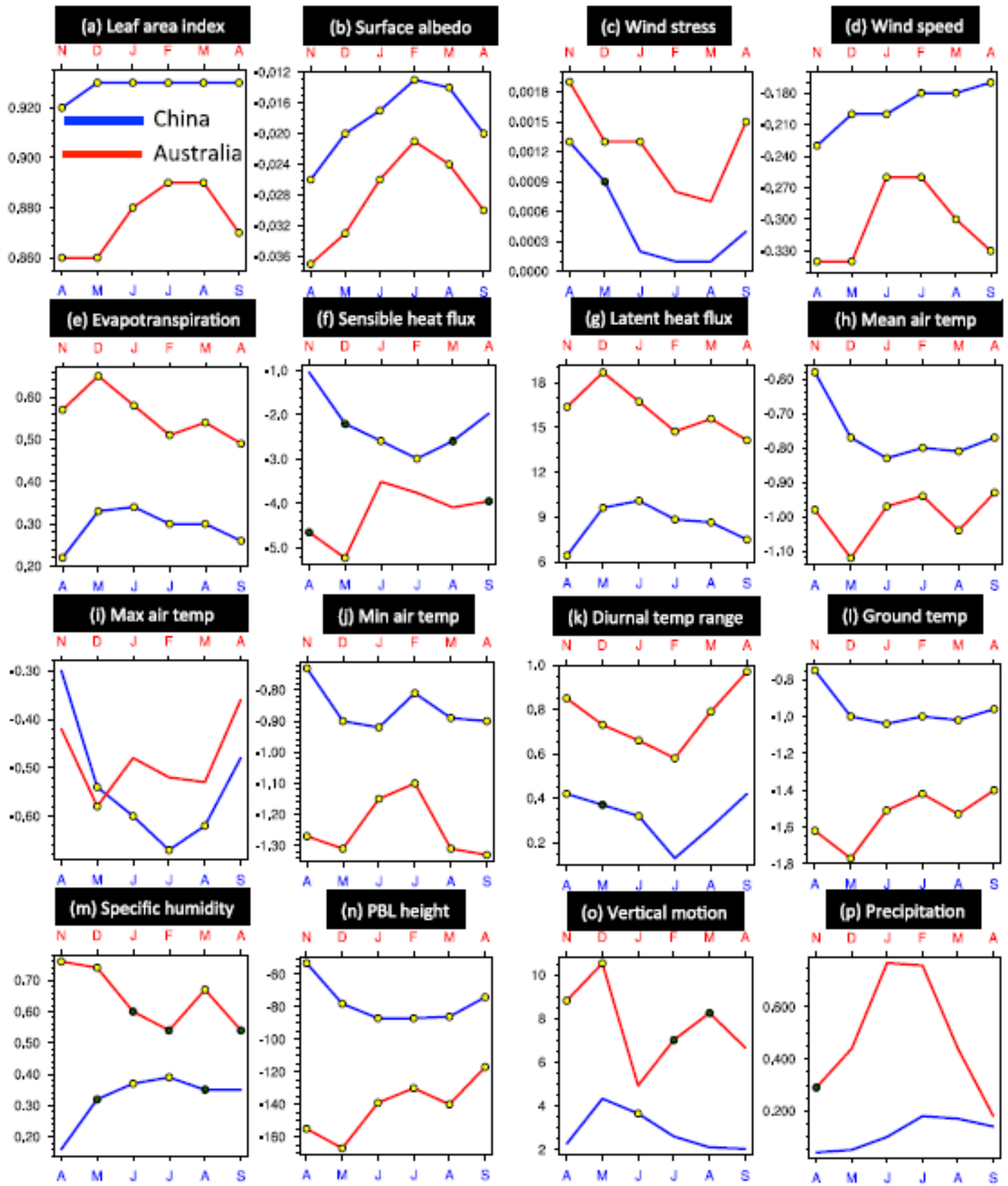

FIG. 9. Local responses in (a) LAI ($m^2\ m^{-2}$), (b) surface albedo (fraction LAI^{-1}), (c) wind stress ($N\ m^{-2}\ LAI^{-1}$), (d) 10-m wind speed ($m\ s^{-1}\ LAI^{-1}$), (e) ET ($mm\ day^{-1}\ LAI^{-1}$), (f) SHF ($W\ m^{-2}\ LAI^{-1}$), (g) LHF ($W\ m^{-2}\ LAI^{-1}$), (h) 2-m mean air temperature ($°C\ LAI^{-1}$), (i) 2-m max air temperature ($°C\ LAI^{-1}$), (j) 2-m min air temperature ($°C\ LAI^{-1}$), (k) DTR ($°C\ LAI^{-1}$), (l) ground temperature ($°C\ LAI^{-1}$), (m) 2-m specific humidity ($g\ kg^{-1}\ LAI^{-1}$), (n) PBL height ($m\ LAI^{-1}$), (o) vertical motion at sigma level 0.83 ($hPa\ s^{-1}\ LAI^{-1}$), and (p) precipitation ($mm\ day^{-1}\ LAI^{-1}$) across the Chinese monsoon region in April–September (blue) and Australian monsoon region in November–April (red) to an LAI increase of $1\ m^2\ m^{-2}$, based on ENSINC minus ENSDEC. Green and yellow dots identify statistically significant differences at $p < 0.1$ and $p < 0.05$, respectively.

Over monsoon regions for China and Australia, greater LAI supports reductions in albedo, temperature, wind speed, boundary layer height, ascending motion, and midlevel clouds and increases in DTR, wind stress, ET, specific humidity, and low clouds. In response to greater LAI, rainfall is enhanced during Australia's pre-to-midmonsoon season but not for China.

He et al., 2017

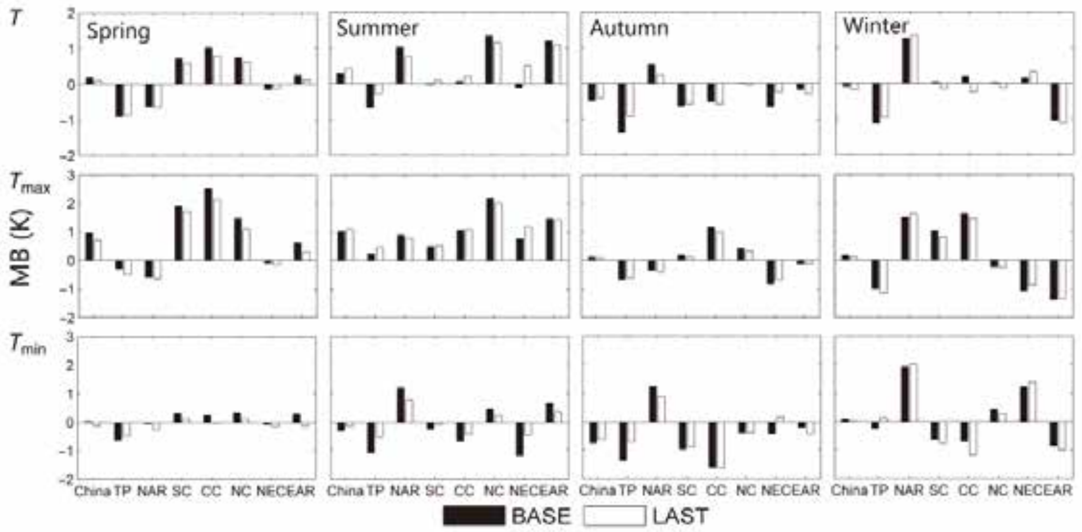

Figure 5. MB of daily mean temperature (T), daily maximum (T_{max}), and minimum (T_{min}) temperature in China and seven sub-regions for four seasons of 2006.

With updated land surface information, WRF's performance in terms of both daily average values and extremes improved. These improvements are significant for temperature, but not significant for precipitation.

Meng et al., 2018

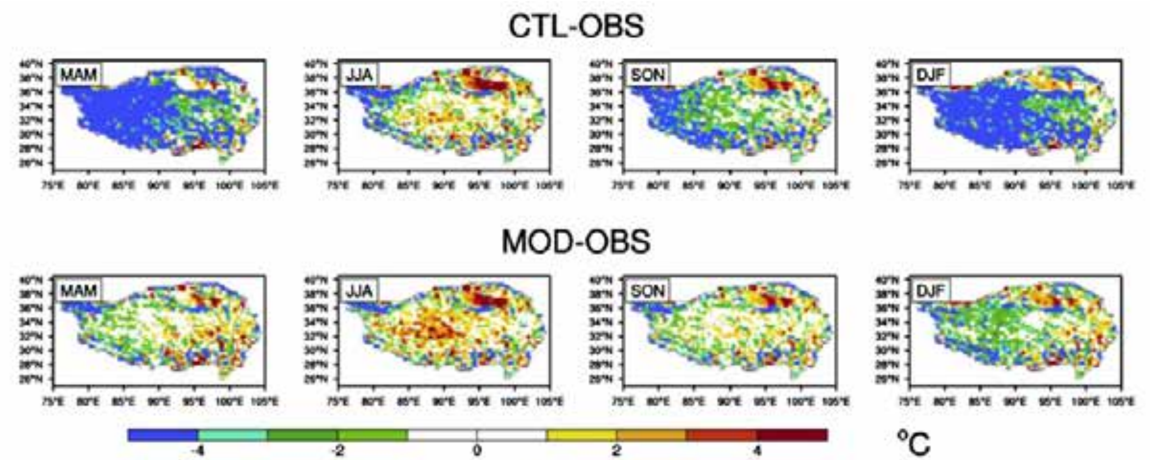

Figure 4. Seasonal distribution of 2 m air temperature from OBS, CTL and MOD, and the differences between the simulations with the observations (i.e. CTL-OBS and MOD-OBS).

Using updated albedo in the WRF Model lower boundary condition demonstrating evident improvement for cold temperature biases in the TP.

Effects of vegetation fraction variation on regional climate simulation over Eastern China

1. What are the impacts of vegetation variations on climate over Eastern China?

2. Will the updated GVF data improve the model's performance?

Outline

- Background & History
- **Vegetation Effects over China**
- Conclusions

Experimental design

Model: WRF v3.6.1

Time: 1982-2011

Simulation	GVF
CTL	NOAA GVI system (Jiang et al., 2010) Fixed seasonal cycle from 1982 to 2011
CLMV	WRF's default GVF (Gutman and Ignatov, 1998) Fixed seasonal cycle from 1985 to 1990
DYNV	NOAA GVI system (Jiang et al., 2010) Monthly GVF from 1982 to 2011

Experiment design

GVF

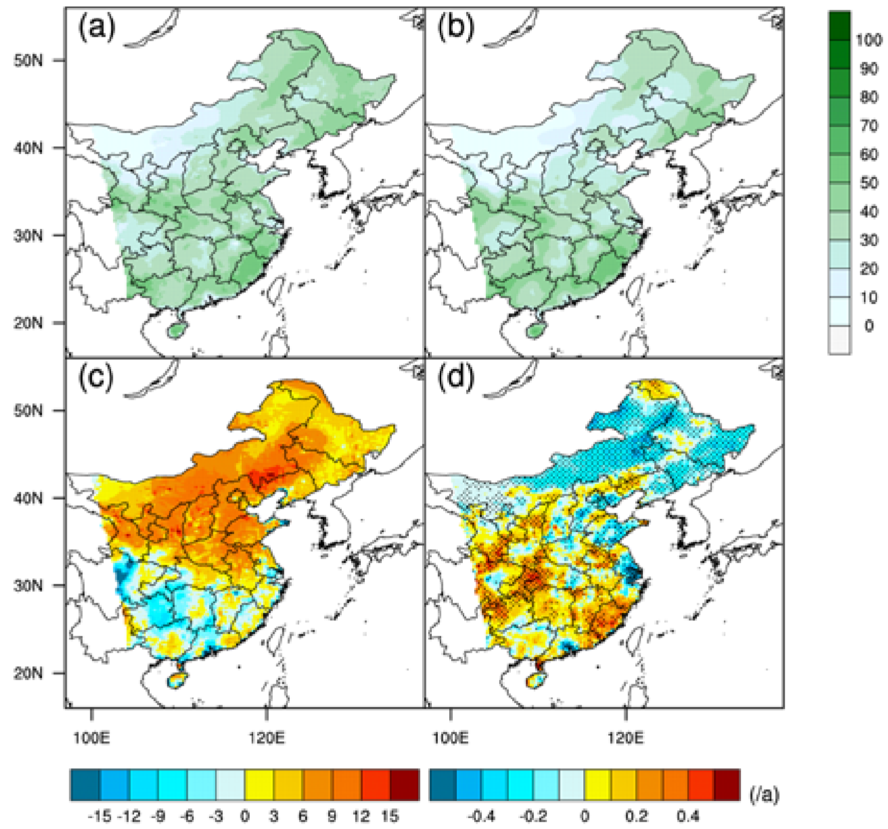

Evaluation of the CTL experiment

Temp **CTL-OBS**

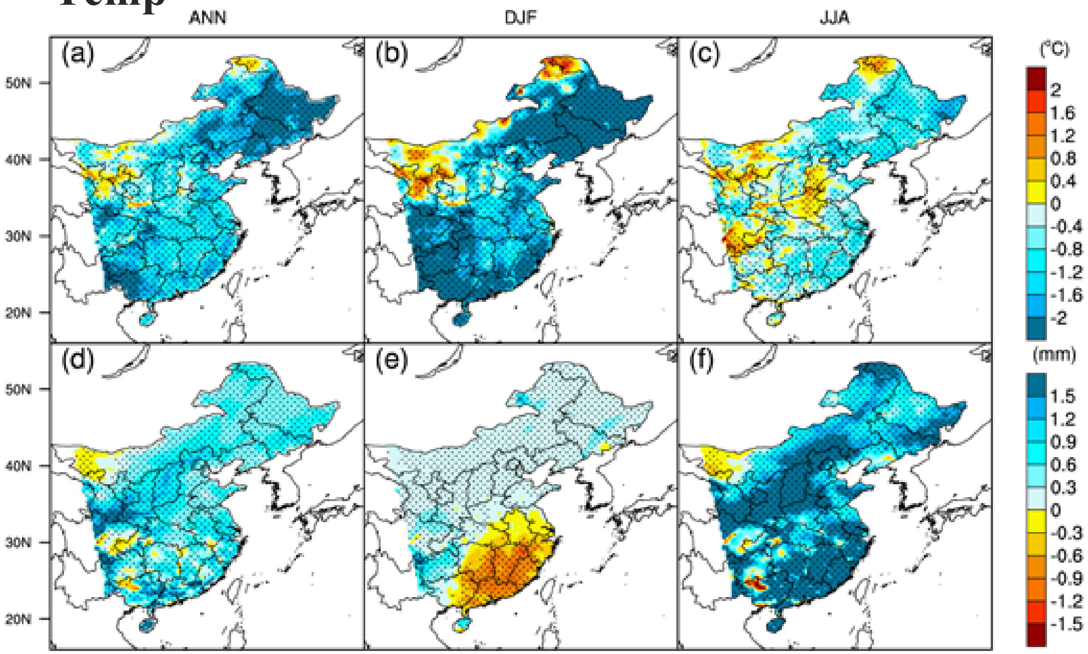

Precip

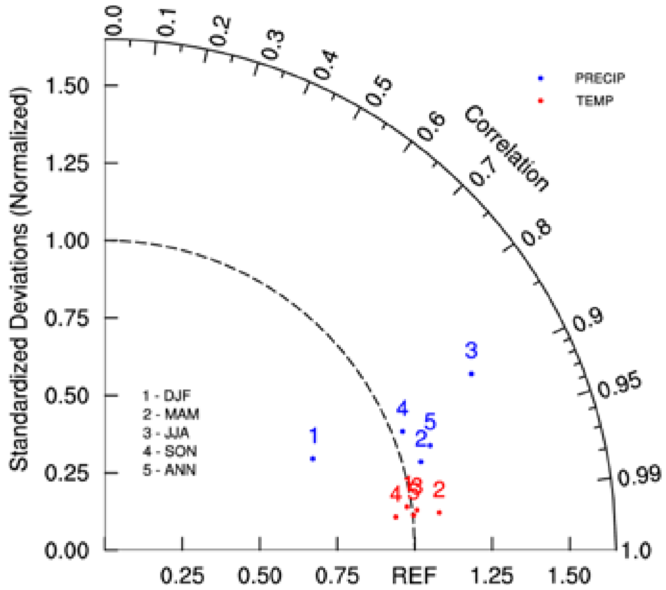

CORR

Temp

Precip

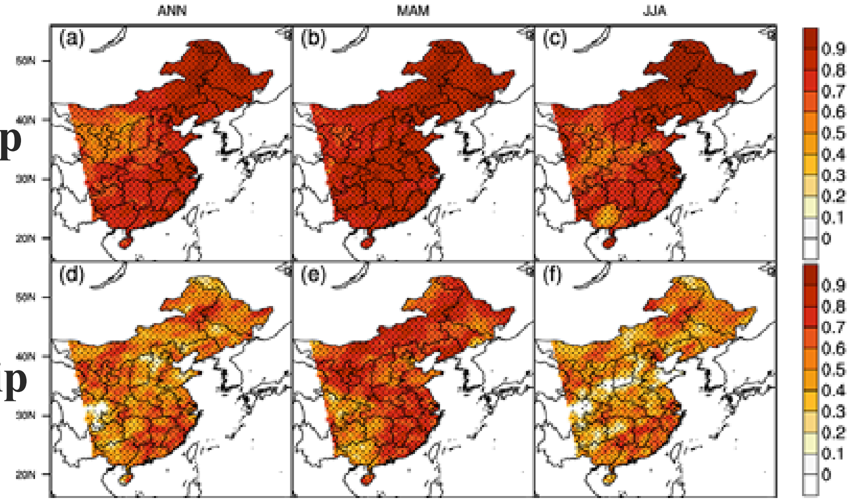

RMSE

Temp

Precip

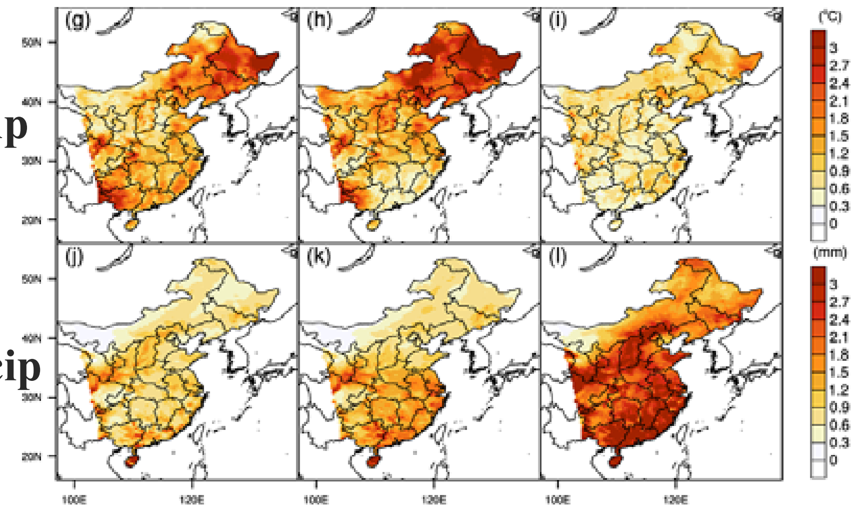

- **Climatology view**

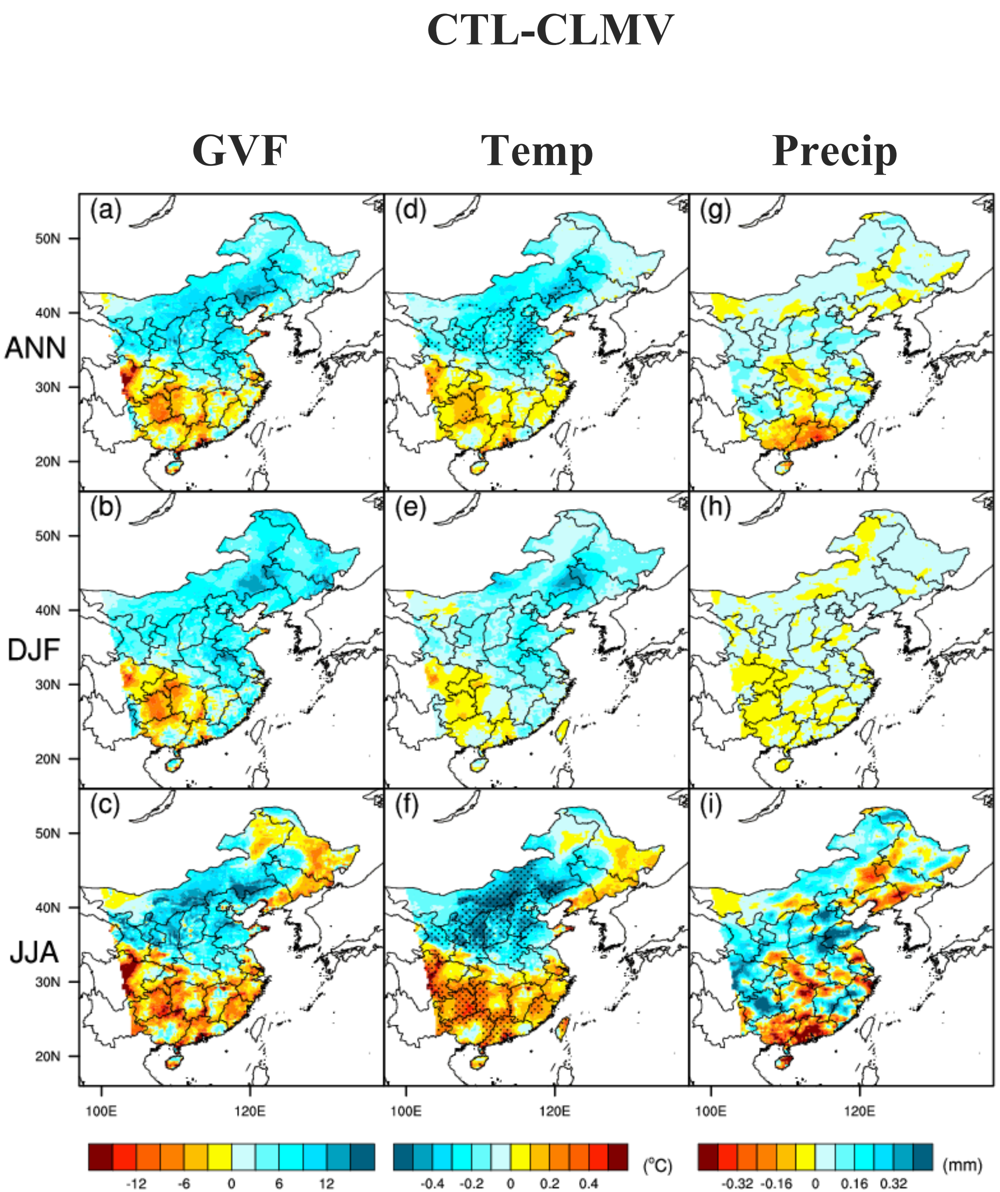

- **Linear trend**

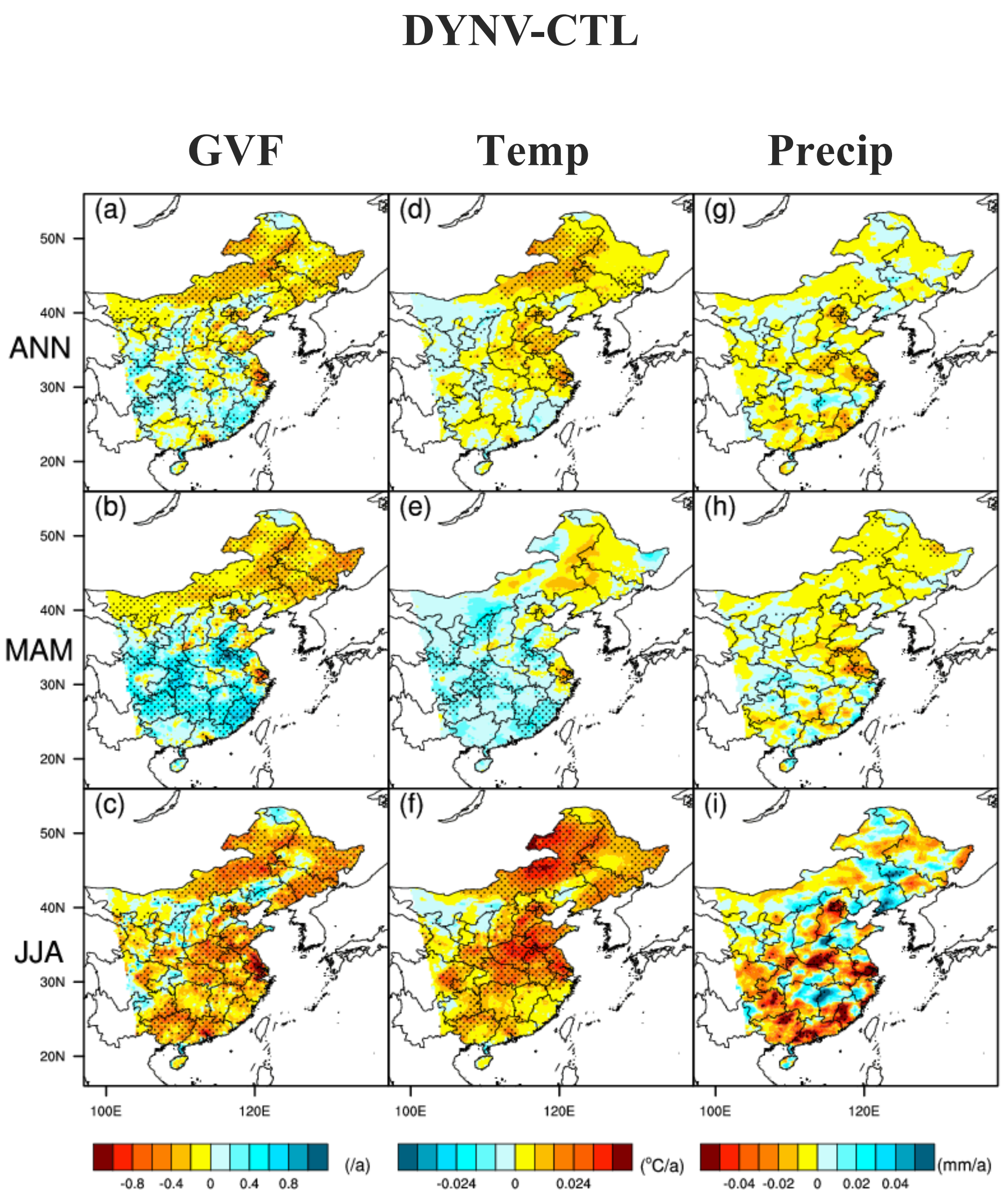

The increase of vegetation will decrease the temperature and vice versa.

• Climatology view

CTL-CLMV

Vegetation Climate Feedback

Radiation Feedback

Radiation Feedback

Mo

M

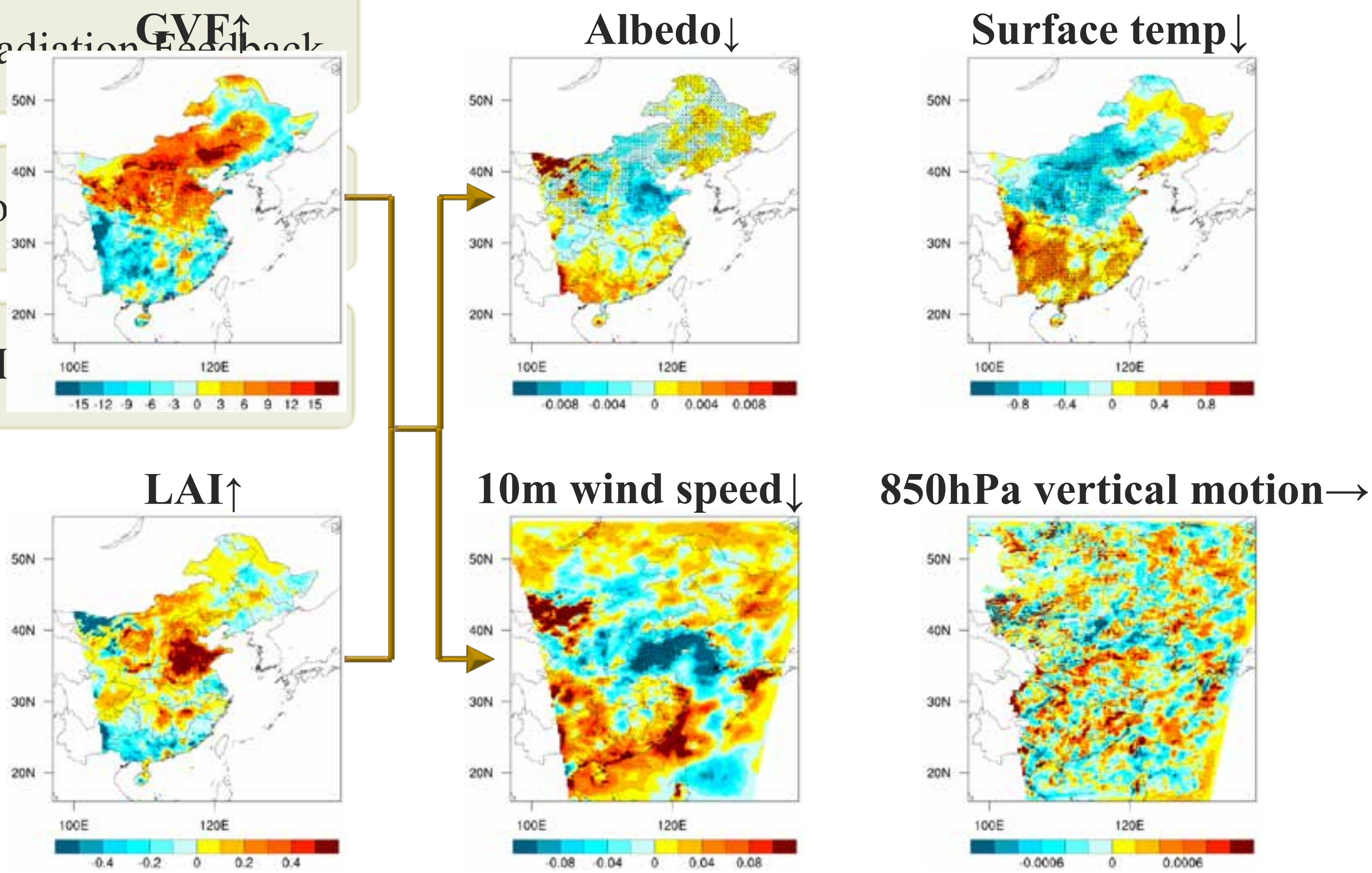

Momentum Feedback

- # Climatology view

CTL-CLMV

Moisture Feedback

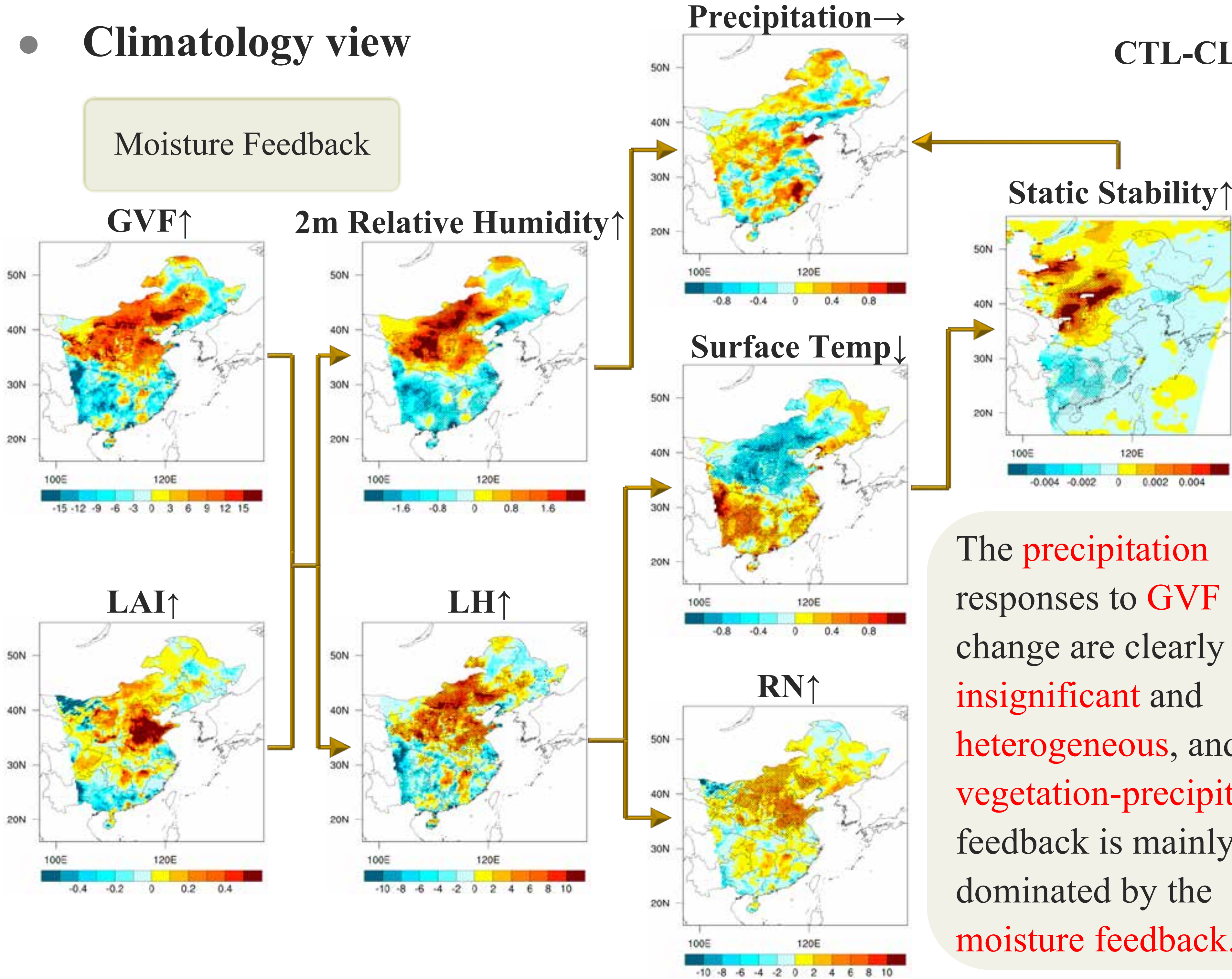

The precipitation responses to GVF change are clearly insignificant and heterogeneous, and the vegetation-precipitation feedback is mainly dominated by the moisture feedback.

Extreme indices and heat wave

Linear trend

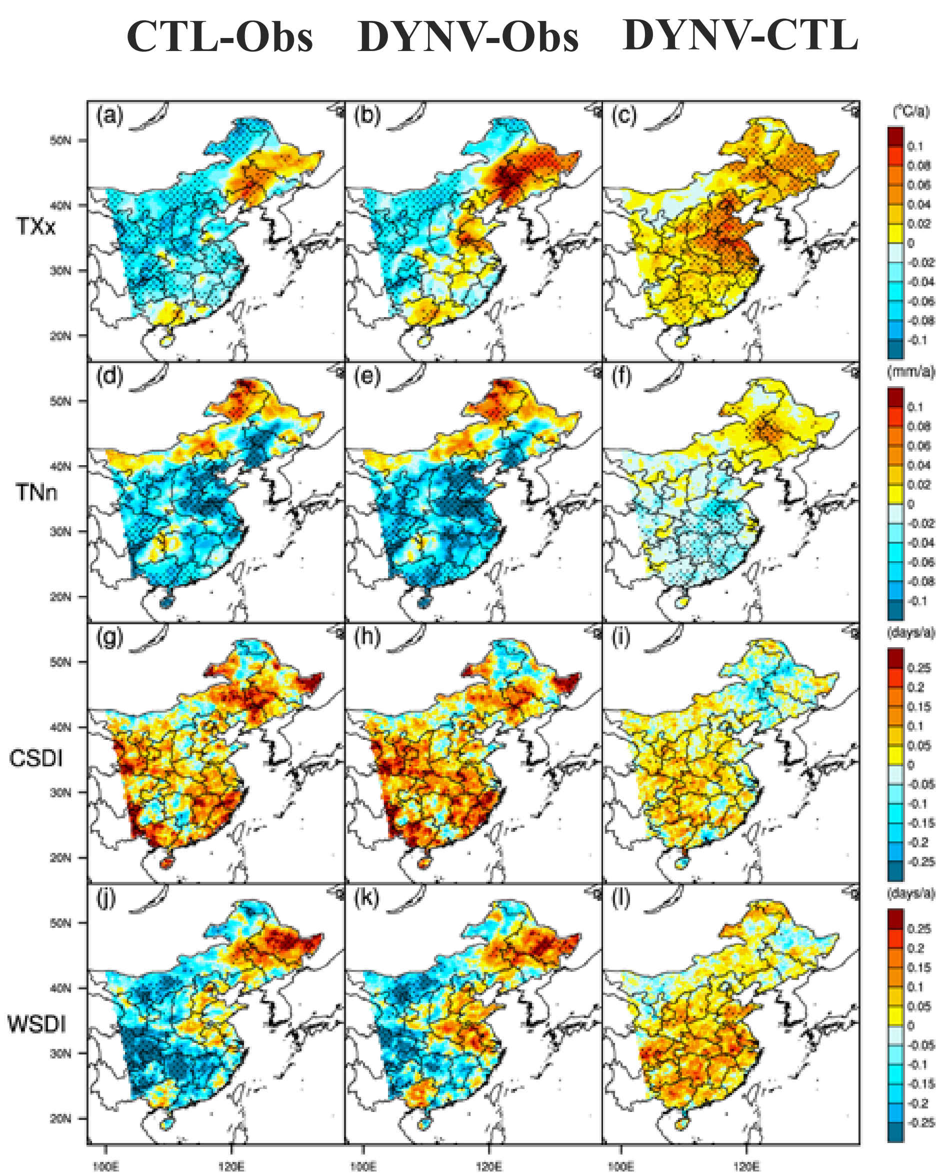

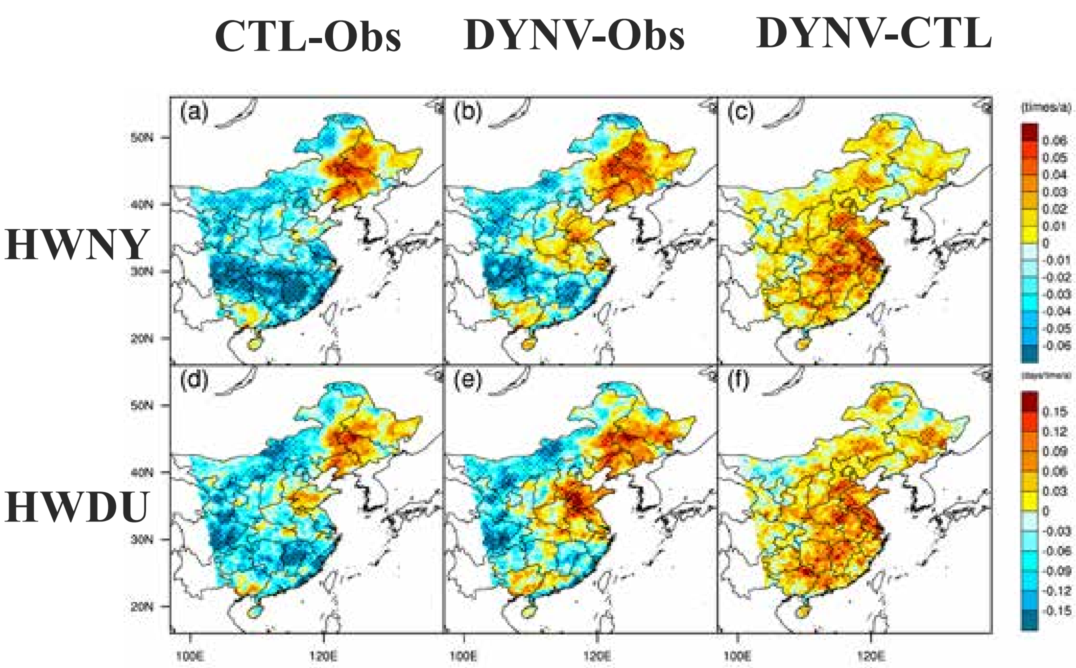

Over regions south of the Yangtze River, the simulation of the interannual variation for the extremes such as TXx, WSDI and heat wave indices have been improved by using dynamic GVF data.

Outline

- Background & History
- Regional vegetation Effects
- **Conclusions**

Conclusions

- Without considering other reasons, the increase of vegetation will decrease the temperature and vice versa.
- In response to GVF change, the results show that the vegetation-climate feedback supports the moisture feedback, dominating over the radiation and momentum feedback.
- For extremes and heat wave, it is detected that the DYNV has better stimulation on TXx, WSDI, HWNY and HWDU than CTL's over most of the Southeast China, although it may introduce some new biases.

Thank You!